Measurement of the contribution of excitation autoionization to electron-impact ionization of ions: Ti^{3+}, Zr^{3+}, Hf^{3+}, and Ta^{3+}

R. A. Falk and G. H. Dunn*
Joint Institute for Laboratory Astrophysics, University of Colorado and National Bureau of Standards, Boulder, Colorado 80309

D. C. Gregory and D. H. Crandall
Physics Division, Oak Ridge National Laboratory, Oak Ridge, Tennessee 37830
(Received 23 August 1982)

Measurements were made of the cross section for electron-impact single ionization of the transition-element ions Ti^{3+}, Zr^{3+}, Hf^{3+}, and Ta^{3+} for an electron-energy range from threshold to 1000 eV. The cross sections are enhanced by as much as a factor of 20 due to excitation autoionization primarily involving $\Delta n=0$ transitions, $np^6nd^m \rightarrow np^5nd^{m+1}$. Comparisons with recent theoretical predictions show reasonable agreement between measured and predicted positions of the autoionization states; however, the magnitudes of the theoretical cross sections are greater than the experimental values by a factor of approximately 2.5.

I. INTRODUCTION

Electron-impact ionization of atoms or ions occurs through a number of mechanisms in addition to the direct "knock-out" process. Excitation of inner-shell electrons to quasibound states above the ionization limit, followed by autoionization can—and often does—contribute a significant part of the total ionization cross section. It has been demonstrated experimentally by Peart *et al.*[1] and by Feeney *et al.*[2] for Ca^+, Sr^+, and Ba^+ that this mechanism, which is usually referred to as excitation-autoionization (EA), can actually be the dominant mechanism in ionization. For example, in the case of Ba^+ the EA contribution to the total ionization cross section appears to be four times as large as the contribution from the direct process. In a recent paper,[3] we previously reported results that showed both experimentally and theoretically that EA can dominate the direct process by more than an order of magnitude, due primarily to excitation of the type $np^6nd^m \rightarrow np^5nd^{m+1}$. Many people[4] have recognized that EA is an important process and must be reckoned with in the modeling of hot plasmas such as encountered in fusion physics and astrophysics. The work reported here and in our earlier paper[3] emphasizes that importance and highlights the need to be able more fully to predict and understand the EA process.

Griffin *et al.*[5] have presented details of, and extension on, the theoretical aspects of EA as presented in Ref. 3. It is the purpose of this paper to present experimental details of the work reported in Ref. 3, and to present data not previously given there, including data at higher energies and data on Ta^{3+}. Comparisons are made with the theoretical estimates of EA and of the direct process.

II. EXPERIMENTAL METHOD

Generally, the experiment was conducted using the crossed-charged-beams technique with the apparatus illustrated in Fig. 1. The apparatus shown in Fig. 1 and the techniques used here have been described in some detail previously.[6] The target ions were extracted from an ion source and formed into a beam which led into a region of ultrahigh vacuum

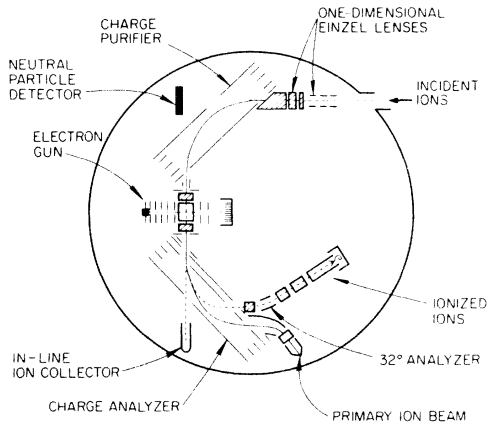

FIG. 1. Schematic of the crossed-beams collision chamber and ion-beam analysis system viewed from above. Cross-hatched elements can provide vertical deflection of ions.

(10^{-9} Torr). Electrons, in a beam at right angles to the ion beam, bombarded the target ions. An electrostatic parallel-plate analyzer separated ions of different charge-to-energy ratio, and thus it separated ions which had undergone ionizing collisions from the primary beam. The primary electron- and ion-beam currents were measured, the product ions counted, geometric overlap of the beams was measured, and the cross section was calculated from the relationship[6,7] basic to colliding-beams experiments:

$$\sigma=\frac{R_{+1}qe^2v_iv_e}{I_iI_e(v_i^2+v_e^2)^{1/2}}\frac{\mathcal{F}}{D_{+1}} . \tag{1}$$

Here I_i, I_e and v_i, v_e are the currents and velocities of the impacting ions and electrons, respectively, q is the charge of the target ions, R_{+1} is the count rate for the product ions of charge $q+1$, and D_{+1} is the probability that an ion of charge $q+1$ produced by electron impact will be detected. The form factor $\mathcal{F}$ takes account of the spatial overlap of the two beams, and is given by

$$\mathcal{F}=\frac{\int R(z)dz\int G(z)dz}{\int R(z)G(z)dz} , \tag{2}$$

where $R(z)$ and $G(z)$ are the relative vertical distributions of the electron- and ion-beam current densities. The electron beam was chopped and detectors appropriately gated to allow separate measurements of background and signal plus background.

The electrons were produced in a gun patterned after the one developed by Taylor *et al.*,[8] the characteristics of which have been studied in detail. The electron-ion interaction energy was determined from

$$E=V_c-\phi-\frac{S}{\sqrt{V_c}}I_e+\frac{m_e}{m_i}(E_i+E_e)+\Delta_F , \tag{3}$$

and the energy spread from

$$\Delta E=\Delta V_{\text{th}}+\frac{S'}{\sqrt{v_c}}I_e+\delta_F . \tag{4}$$

Here V_c is the potential difference between the gun cathode and the interaction region, ϕ is a contact potential, S and S' are geometric factors allowing for calculation of space-charge effects, E_i and E_e are the laboratory energies of ions and electrons which have masses m_i and m_e, respectively, and ΔV_{th} is the thermal spread of electron energies from the cathode. The quantities Δ_F and δ_F are an energy shift and spread, respectively, due to the penetration into the interaction region of electric fields from deflector plates shown in Fig. 1, located both before and after the electron gun along the ion beam in such a way to compensate for the deflection of the ions by the 0.02-T magnetic field of the electron gun. The quantities Δ_F and δ_F are, in these experiments, the least-well-defined quantities in Eqs. (3) and (4), and lead to the largest uncertainties in E and ΔE. The energy E is known to ± 0.4 eV from Eq. (3). The energy width is assessed to be about 2 eV, and is dominated by the term δ_F.

Ions were made in the ORNL-PIG, a cold cathode Penning discharge source, which has been described[9] earlier. For Ti^{3+}, Zi^{3+}, and Ta^{3+} an arc was struck in a gas mixture of CCl_4 seeded with Xe. Metal samples of Ti or Zr in the form of foils rolled into small cylinders were introduced into the discharge region through the anode cylinder wall opposite the extraction slit. Ta was normally present in ion source parts (cathodes and exit slit). Chlorine from CCl_4 combined with the metals, forming the metal chloride, which has a high vapor pressure at the temperature of the walls of the ion source. The source was thereby effectively seeded with the desired metal. Only unusably small amounts of Hf^{3+} could be obtained by this method, however. Therefore, Hf was introduced directly into the source via a heated reservior containing $HfCl_3$. The ions were extracted at a potential of 10 keV and typical ion currents were 1—20 particle nanoamperes, though only a few tenths of a nanoampere of Ta^{3+} could be obtained.

As shown in Fig. 1, the ions undergo a 90° deflection in an electrostatic field just prior to entering the collision box. This eliminates ions of different charge-to-energy ratio which have come into the beam via charge transfer along the beam-transport system. However, there may still be ions from the source which have the same charge-to-mass ratio but are not the same ion. For example, the anode of the ion source was copper, and Cu^{4+} and Ti^{3+} have nearly the same charge-to-mass ratios. The extent of such contamination was assessed by introducing gas into the vacuum region just prior to the main chamber of Fig. 1. Then, sweeping the voltage on the "charge purifier," the components of charge-transferred ions can be identified as they are transmitted to the "in-line collector." Ions of different initial charge in the primary beam give sequences of charge-transferred peaks, the relative intensities of which can be used to obtain approximate intensities of the individual parent-ion components. It was shown that impurity ions were totally negligible for Zr^{3+} and Hf^{3+}. For Ti^{3+}, it was found that there was often a small component of O^+ in the beam. This was observed and assessed with the charge-transfer technique described above, except a neutral-particle detector shown in Fig. 1 was used to detect the resultant O atoms. This contamination was kept below 2%, and corrections were made to

the data. No assessment was made by this technique for Ta^{3+}. Other "impurities" in the ion beams can be metastable states of the target ions. By examining the cross sections below the threshold for ionization of the ground state, and using Lotz-formula[10] estimates for ionization from metastable states, we estimated that in all cases the metastable content of the beams was less than 10%.

Typically, data were obtained using computer control to measure beam distributions [Eq. (2)], record signal and incident-beam currents, and to change the energy. Normally, a range of energy was selected over which $\mathcal{F}$ [Eq. (2)] did not vary by more than 3%. This range was divided into distinct energies at which data were to be obtained. Form factors were obtained at the beginning, end, and middle of the interval, and values of $\mathcal{F}$ were interpolated for intermediate energies. Data were obtained at an energy, the computer stepped to the next, and so on until measurements were obtained at all chosen energies in the interval. The sequence was repeated a selectable number of times until sufficiently precise data were obtained as determined by the standard deviation of the means of the combination of measurements at a given energy. Included in each measurement set were measurements at a benchmark energy (293 eV), so that all data in every energy interval were related to measurements at this benchmark. Careful absolute calibrations were made at the benchmark energy, and all data were thus put on an absolute scale.

The error budget is shown in Table I. Uncertainties are shown at what is believed to be equivalent to the 68% confidence level (1σ). Total uncertainty is computed as a quadrature sum of statistical uncertainty and estimated systematic uncertainties, except that one-sided uncertainties are added linearly.

III. RESULTS AND DISCUSSION

The experimental values of the cross sections for ionization of Ti^{3+}, Zr^{3+}, Hf^{3+}, and Ta^{3+} are tabulated in Table II. The uncertainties shown in parentheses are the counting statistics for the data, and are one standard deviation of the mean. The first entry in the error budget, Table I, is taken as representative of these uncertainties, except that the Table I entry is quoted in percent. As noted earlier, energies are uncertain by ± 0.4 eV.

Figures 2–4 show the cross section plotted versus energy, covering about the first 10 eV above threshold. Also shown in the figures are dashed curves which represent calculations using the Lotz formula[10] for the direct-ionization cross section. As will be discussed in more detail later, these Lotz-formula estimates probably represent an upper limit for the cross section for the direct process. In every case, the measured cross section is significantly larger

TABLE I. Experimental uncertainties quoted at one standard deviation. Systematic uncertainties judged to have a possible correlation were added linearly after which a quadrature sum was made. One-sided systematic uncertainties were added linearly to the resultant quadrature sum.

Source	Uncertainty (in %) Ti^{3+}	Zr^{3+}	Hf^{3+}	Ta^{3+}
Statistical uncertainty				
typical value in % of peak value	±3	±3	±4	±8
Systematic uncertainties				
Particle counting efficiency	±1	±1	±1	±1
Transmission to signal ion counter	±3	±3	±3	±3
Background modulation	±1	±1	±1	±1
Incident-ion current	±1	±1	±1	±1
Incident-electron current	±1	±1	±1	±1
Form-factor evaluation[a]	±2	±2	±2	±2
Uncertainty in velocities	±1	±1	±1	±1
Ion-beam contamination	±2			
Total systematic	+6 −4	+4	+4	+4
Total % uncertainty (typical)	+7 −5	±5	±6	±9

[a]Some form factors in the Ta^{3+} measurements had uncertainties ranging to 7%. These have been included in the uncertainties quoted in Table II and shown in Fig. 8.

TABLE II. Measured cross sections for single-electron ionization of Ti^{3+}, Zr^{3+}, Hf^{3+}, and Ta^{3+} by electron impact. Values in parentheses are one standard deviation counting statistics and are taken as representative of relative uncertainties.

Target	E (eV)	σ (10^{-18} cm^2)	E (eV)	σ (10^{-18} cm^2)	E (eV)	σ (10^{-18} cm^2)	E (eV)	σ (10^{-18} cm^2)	E (eV)	σ (10^{-18} cm^2)	E (eV)	σ (10^{-18} cm^2)	E (eV)	σ (10^{-18} cm^2)
Ti^{3+}	43.4	3.2(2.3)	49.3	30.3(1.5)	55.3	37.41(1.2)	61.2	46.4(1.3)	67.1	53.5(1.2)	95.6	60.3(1.4)	263	55.9(1.0)
	43.8	6.5(1.0)	49.8	30.6(1.7)	55.8	35.6(1.2)	61.7	47.4(1.0)	67.6	52.8(1.2)	96.1	60.9(1.0)	293	52.9(0.1)
	44.4	12.3(2.0)	50.3	28.1(1.4)	56.3	38.9(1.0)	62.2	47.5(1.1)	68.1	53.4(1.3)	101	64.1(1.2)	392	46.6(0.3)
	44.9	11.6(2.0)	50.8	31.0(1.5)	56.8	39.0(1.0)	62.7	48.8(1.4)	68.6	53.9(1.6)	110	67.9(2.5)	491	42.7(0.4)
	45.3	14.5(1.4)	51.3	31.8(1.4)	57.3	40.9(1.5)	63.2	48.0(1.4)	69.1	53.6(1.4)	115	65.2(1.3)	591	38.9(0.5)
	45.7	14.0(0.8)	51.8	33.5(1.4)	57.8	41.0(1.7)	63.7	50.2(1.3)	69.6	54.2(1.9)	121	64.4(1.7)	689	33.5(0.3)
	46.4	17.0(1.4)	52.3	33.6(1.4)	58.3	42.2(1.2)	64.2	49.4(1.2)	70.1	55.0(1.4)	135	63.3(1.1)	838	28.8(0.2)
	46.8	19.2(1.4)	52.8	33.6(2.0)	58.7	41.2(1.2)	64.7	50.2(1.3)	70.6	56.5(1.4)	145	62.5(0.6)	987	27.2(0.2)
	47.4	21.9(1.3)	53.3	34.4(1.4)	59.3	42.0(0.9)	65.2	49.2(1.5)	76.1	59.6(1.6)	165	61.7(0.8)		
	47.9	24.9(1.3)	53.8	33.6(1.4)	59.7	44.2(0.9)	65.7	51.4(1.4)	80.9	56.7(1.9)	194	59.4(0.5)		
	48.3	29.0(1.3)	54.3	36.3(1.5)	60.2	44.3(1.4)	66.2	52.3(1.4)	85.9	64.7(3.8)	234	56.5(0.6)		
	48.8	30.6(1.3)	54.8	36.0(1.3)	60.7	44.9(0.9)	66.7	51.6(1.8)	90.7	58.0(2.6)	243	53.6(0.8)		
Zr^{3+}	34.9	2.5(1.3)	38.5	59.2(3.5)	44.4	123.6(6.4)	51.3	146.0(4.4)	66.1	148.3(2.6)	95.6	142.2(2.5)	591	65.0(2.9)
	35.3	9.7(3.2)	39.5	79.8(3.8)	45.4	110.5(6.4)	53.4	139.3(4.3)	70.0	140.2(2.2)	120	135.2(3.0)	690	56.2(1.7)
	35.6	12.6(4.2)	40.5	95.5(4.5)	46.4	120.0(4.3)	56.3	143.4(3.1)	70.9	150.8(4.7)	145	130.3(2.7)	839	48.9(1.9)
	36.3	18.6(3.2)	41.5	101.2(2.6)	47.4	116.2(4.8)	58.0	144.9(4.1)	71.9	134.9(1.8)	194	114.7(2.1)	988	447.4(1.4)
	36.5	20.9(3.0)	42.4	106.4(6.2)	48.4	115.0(6.4)	60.0	141.7(5.7)	73.0	153.7(4.8)	293	98.5(0.6)		
	37.3	29.1(3.1)	43.1	108.3(5.9)	49.4	123.0(6.1)	62.0	152.9(4.8)	73.9	144.3(4.2)	392	77.5(1.4)		
	37.6	39.7(3.5)	43.4	110.2(6.2)	50.3	140.3(6.1)	64.0	149.2(5.0)	76.0	151.9(4.2)	491	76.9(1.8)		
Hf^{3+}	33.3	7.3(1.9)	39.2	60.6(4.1)	45.1	90.1(2.3)	53.0	101.3(2.2)	61.0	110.2(2.0)	115	121.4(2.6)	491	85.1(0.4)
	34.2	11.6(2.0)	39.6	58.9(1.3)	46.1	94.0(2.2)	54.0	104.02(2.7)	61.9	114.7(1.9)	120	122.3(1.8)	592	76.6(0.8)
	35.3	22.2(2.3)	40.1	63.6(1.2)	47.1	94.8(2.1)	55.0	104.6(3.1)	62.9	112.1(2.4)	146	119.2(1.1)	690	70.8(0.3)
	35.7	21.0(1.3)	40.6	67.1(1.8)	48.0	89.7(2.2)	56.0	101.5(3.7)	66.2	113.1(3.3)	169	114.5(0.8)	839	64.9(0.3)
	36.2	23.2(1.4)	41.2	72.5(2.0)	49.0	92.8(2.7)	57.0	103.2(1.9)	70.8	118.0(1.9)	194	113.4(0.8)	988	60.6(0.5)
	36.7	30.1(1.3)	42.1	80.0(1.9)	50.1	94.8(1.8)	58.0	103.4(2.1)	75.7	120.7(1.8)	243	101.2(1.0)		
	37.2	33.6(1.2)	43.1	85.5(3.0)	51.1	93.5(1.8)	58.9	109.2(3.1)	80.7	116.6(2.8)	293	100.1(0.4)		
	38.2	46.7(1.2)	44.1	90.3(2.5)	52.0	96.4(2.3)	59.9	109.9(2.1)	96.1	122.9(1.2)	392	90.5(0.7)		
Ta^{3+}	36.3	10.6(4.6)	65.9	101.3(6.9)										
	38.2	17.3(8.4)	80.7	130.2(11.0)										
	40.1	55.8(9.2)	95.4	119.0(8.2)										
	41.0	59.7(7.9)	120	129.0(10.0)										
	46.1	75.5(4.6)	293	104.5(4.2)										
	56.0	117.1(10.7)												

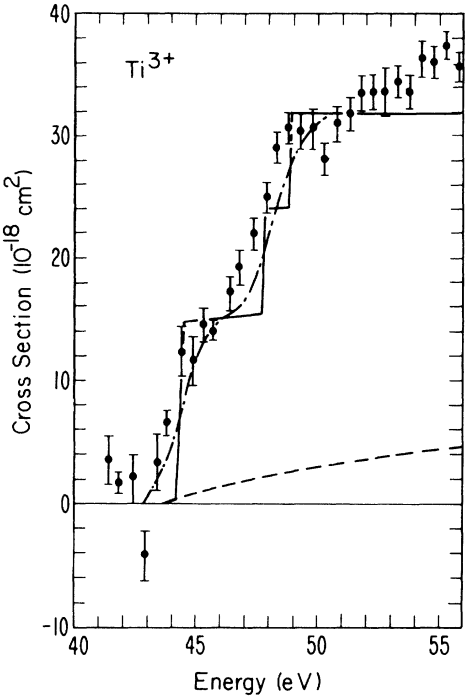

FIG. 2. Cross section in the threshold region for electron-impact ionization of Ti^{3+}. Points, experimental measurements; solid line, DW, dipole approximation calculations from Ref. 5, added to dashed curve; dot-dashed, solid curve convoluted with a 2-eV-FWHM Gaussian to simulate electron-energy distribution; dashed curve, calculated direct-ionization cross section using the Lotz formula [Eq. (6)]. Bars represent counting statistical uncertainties at one standard deviation (1σ).

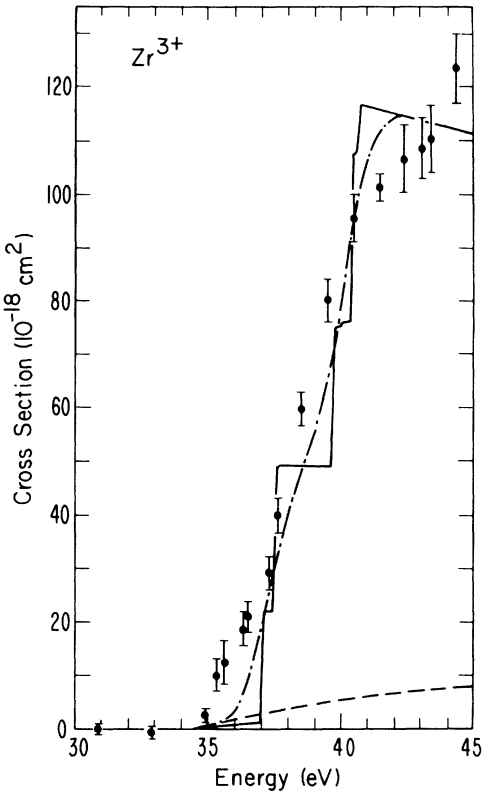

FIG. 3. Cross section in the threshold region for electron-impact ionization of Zr^{3+}. Legend is as in Fig. 2.

than the estimates of the cross section for the direct process. The difference is attributed to excitation-autoionization reactions of the type

$$e+X^{+q}(ns^2np^6nd)\rightarrow X^{+q}(ns^2np^5nd^2)+e \rightarrow X^{+(q+1)}(ns^2np^6)+2e\ . \quad (5)$$

Griffin *et al.*[3,5] have estimated the cross sections for the excitation step of this process using a distorted-wave dipole approximation. They also estimated the branching ratios for excited state autoionization and found nearly all of them close to unity. The resultant EA cross sections, when added to the Lotz-formula estimates for the direct process are all about 2.5 times larger than the observed total ionization cross sections. Their calculated values have been multiplied by 0.4, added to the Lotz-formula cross sections, and plotted in Figs. 2–4 as the solid curves. In turn, these cross sections have been convoluted with a 2-eV-FWHM Gaussian representing the experimental electron-energy spread. The resultant "expected" cross sections are shown by the chain curves in the figures.

In examining the data in Fig. 2 for Ti^{3+} one sees two prominent structures at approximately 44.5 and 47.5 eV. These features are identified[3,5] as excitation autoionization due to the

$$3p^5 3d^2[0.72(^3F)+0.69(^1G)]^2F$$

term at 44.5 (calculated energy), and the experimentally unresolved terms

$$3p^5 3d^2[0.87(^3P)+0.39(^1D)+0.31(^1S)]^2P$$

at 48.0 eV and

$$3p^5 3d^2[0.85(^3F)+0.34(^3P)+0.41(^1D)]^2D$$

at 49.1 eV corresponding to the three steps in the solid theoretical curve in Fig. 3. The convoluted curve agrees quite well with the data, so that except for the factor of 0.4 by which the theoretical results were multiplied, there is reasonable agreement between theory and experiment. In examining Fig. 3 for Zr^{3+}, similar agreement is found, keeping in mind the same scaling factor of 0.4 and the fact that the excited levels are close enough to each other that no real structure is seen in the data. Figure 4 for Hf^{3+} shows much worse agreement between experi-

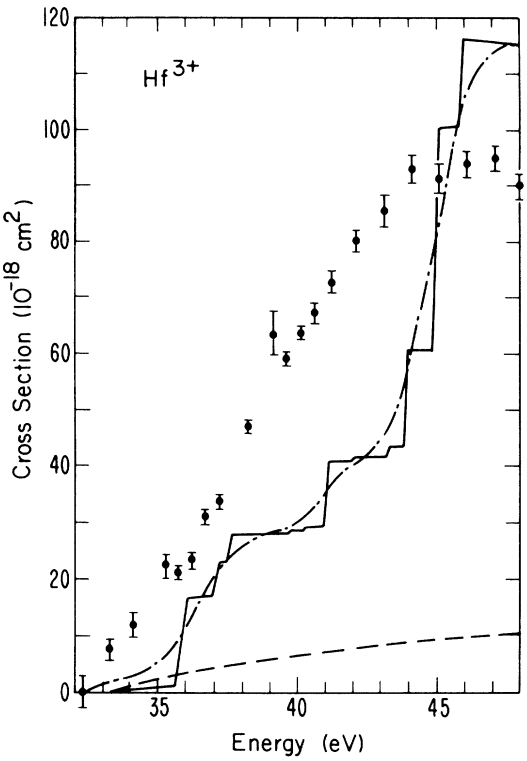

FIG. 4. Cross section in the threshold region for electron-impact ionization of Hf^{3+}. Legend is as in Fig. 2.

ment and the scaled theory. Griffin *et al.*[5] point out a number of shortcomings of their theory, emphasizing their work as preliminary and providing a guide for making a survey of the elements for which EA may be dominant. It was stated that the factor-of-2.5 disparity in magnitude may be associated with a number of things: neglect of exchange, nonunitarized matrix elements, neglect of configuration interaction, and neglect of the role of many states due to use of the dipole approximation. In fact, they report[11] that in subsequent work the inclusion of exchange and higher-order poles makes a substantial improvement in the magnitude of the theory compared with experiment. Thus, one expects improvement in agreement between experiment and theory as the theory is refined. Meanwhile, it is significant that the transition, their energy locations, and their general magnitudes have been identified. It does give a basis for examining other ions to predict similar large effects of EA, and Griffin *et al.*[5] survey a number of other transition-element ions in their work.

Possible contributions to the ionization cross section by recombination resonances which decay via double autoionization[12,13] have not been included in the analysis of the present data. Such resonances occur as Rydberg series below each of the excited states and would correspond to transitions of the form

$$e + X^{+q}(ns^2np^6nd) \rightarrow X^{+(q-1)}(ns^2np^5nd^2, n'l) \rightarrow X^{+(q+1)}(ns^2np^6) + 2e \ .$$

Within typical energy spacings of such resonances and our energy resolution, the effect of such resonances should be to broaden and shift the observed excitation-autoionization components toward lower energies.[13] Indeed, there is some small indication of such broadening and shift in the present experiment compared to the excitation-autoionization calculations. However, well-separated resonances, for n' close to n, are likely to be bound states in the present experiment and would not decay by double autoionization. It is not clear that resonances need to be invoked to explain present data relative to the available calculations. Nevertheless, we point out their possible contribution in the present data. It is not likely that such resonances would account for the factor-of-2.5 discrepancy in magnitude between experiment and calculations.

The cross sections in Table II are presented in their entirety in Figs. 5–8. The cross sections for Ti^{3+}, Zr^{3+}, and Hf^{3+} continue to climb past the energies for exciting np^5nd^2 levels. It is quite probable that other EA transitions associated with excitation to $np^5nd(n+1)p$, $np^5nd(n+1)d$, and $nsnp^6nd^2$ levels play a role in this continuing rise.

Plotted with the data in Figs. 5–8 are two sets of curves. The dashed curves are, as in Figs. 2–4, cross sections calculated using the Lotz formula.[10] The solid curves are calculated using the scaled

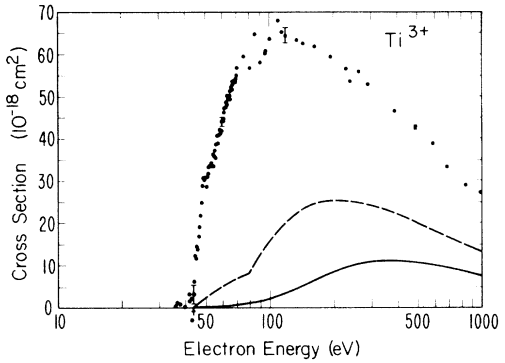

FIG. 5. Cross section vs interaction energy for electron-impact single ionization of Ti^{3+}. Representative bars show counting statistical uncertainties at 1σ. Dashed curve is the prediction using the Lotz formula [Eq. (6)] for the cross section for direct knock-out ionization. Solid curve is the prediction using the SPWBA method of McGuire (Ref. 14) for the direct process. See discussion in text of Lotz parameters for *d*-subshell electrons.

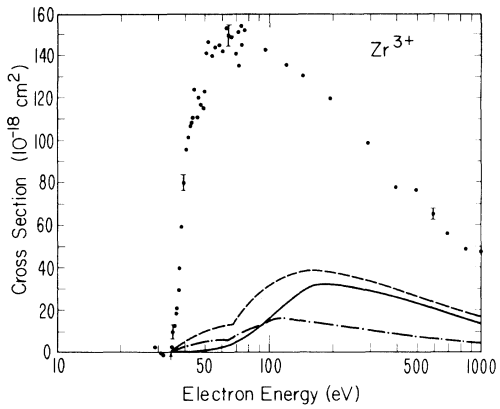

FIG. 6. Cross section vs interaction energy for electron-impact single ionization of Zr^{3+}. Legend is as in Fig. 5. Dot-dashed curve is the prediction using the SCB method of Golden and Sampson (Ref. 13) for the direct process.

plane-wave Born-approximation (SPWBA) method of McGuire[14] which should be of limited applicability for ions. Shown only in Fig. 6 for Zr^{3+} is a curve calculated using the method of Sampson and Golden,[15] the so-called scaled Coulomb-Born (SCB) method. This latter approximation was not used for all the cases, since these ions are not nearly highly enough charged for SCB to be valid within the criteria given by its authors.[15] As stated earlier, the Lotz-formula estimates seem to be an upper limit for the direct process. Most experimental data to date seem to bear this out[6,16] also.

In constructing the curves of Figs. 2–8, ionization energies of the different subshells calculated by Griffin[17] were used. These are tabulated in Table III, since they do not seem to be readily available in the literature.

The Lotz formula[10] can be written

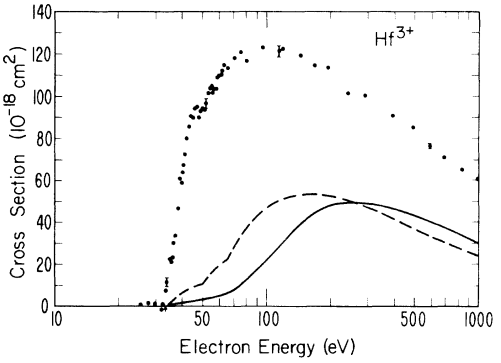

FIG. 7. Cross section vs interaction energy for electron-impact single ionization of Hf^{3+}. Legend is as in Fig. 5. See discussion in text of the Lotz parameters for f-subshell electrons.

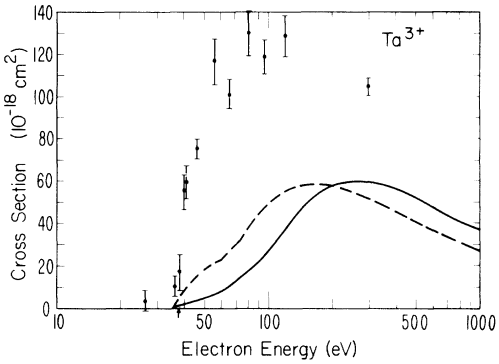

FIG. 8. Cross section vs interaction for electron-impact single ionization of Ta^{3+}. Legend is as in Fig. 5. See discussion in text of the Lotz parameters for f-subshell electrons.

$$\sigma = \sum_{i=1}^{N} a_i q_i \frac{\ln(E/P_i)}{EP_i} \times \{1 - b_i \exp[-c_i(E/P_i - 1)]\} , \quad (6)$$

where E is the impact energy, P_i is the binding energy of the electrons in the ith subshell, q_i is the number of electrons in the ith subshell, and a_i, b_i, and c_i are constants which have been tabulated for a large number of atoms and ions by Lotz by comparison with experiment and/or theory. Lotz had only the case of ionization of neutral mercury for data to help deduce coefficients for d-shell electrons. Generally, for species containing d electrons, he recommended a $\approx 4.5 \times 10^{-14}$ cm^2, a number he recommended for "universal" use when no data were available to indicate otherwise. In constructing the curves in Figs. 2–8, this value was used for the d electrons, even though recent evidence[18,19] suggest that the value should be about half as large. For the best estimate of direct ionization using the Lotz formula, we would recommend a value of a_d about one-half the value used here, but in the present case we emphasize the "upper-limit" nature of the

TABLE III. Ionization threshold energies (in eV) for removal of electrons from specific subshells of the ion species studied here. Data are from Griffin.[5]

Ti^{3+}	3d	3p	3s	
	43.1	77.4	109.9	
Zr^{3+}	4d	4p	4s	
	34.3	64.4	94.0	
Hf^{3+}	5d	4f	5p	5s
	33.2	49.7	65.6	105.7
Ta^{3+}	5d	4f	5p	5s
	34.8	61.7	75.4	113.7

dashed curve. Futhermore, it should be noted that if electrons in the $3s$, $4s$, or $5s$ subshells of Ti^{3+}, Zr^{3+}, or Hf^{3+} are knocked out in direct ionization, further Auger ionization can occur leaving a $5+$ ion which would not be detected in the present experiments. Since these subshells were included in construction of the curves in the figures, the upper-limit nature of the curves is further emphasized.

In dealing with f-subshell electrons, there are no recommedations by Lotz for coefficients. If his universal $a = 4.5 \times 10^{-14}$ cm^2 were adopted, then in Fig. 7 for Hf^{3+} one would see a rise starting at 49.7 eV and going to $\sim 200 \times 10^{18}$ cm^2 at ~ 175 eV—an increase of about 120×10^{-18} cm^2. The increase is about six times less than this. In fact, if one uses the McGuire[14] SPWBA predictions as a guide, then $a_f \approx 0.75 \times 10^{-14}$ for Hf^{3+} and $a_f \approx 1.1 \times 10^{-14}$ for Ta^{3+}. These were the numbers used for f electrons in constructing the dashed curve from Eq. (6). The rise past 50 eV in Fig. 7 is taken as good evidence that these numbers for a_f are reasonable.

The data for Ta^{3+} are both more sparse and of less precision than those for the other three species. This is due, mainly, to the fact that only 0.2—0.3 nA of Ta^{3+} could be obtained in the beam, and the beam could not be maintained for the extended time periods needed for precise data. There are no EA calculations with which to compare. However, it is clear from Fig. 8 that EA totally dominates ionization near threshold, and is at least as large as the direct process at high energies. The Ta^{3+} data are similar in these respects to those for the other species studied here.

In conclusion, the cross sections for electron-impact single ionization of Ti^{3+}, Zr^{3+}, Hf^{3+}, and Ta^{3+} have been measured and presented here. Comparisons of the data with reasonable estimates of the cross section for direct ionization of these species indicate that excitations of the type $np^6nd \rightarrow np^5nd^2$, followed by autoionization, totally dominate the ionization cross section for $E/P \lesssim 1$. Distorted-wave dipole estimates by Griffin *et al.*[5] of this EA are in good agreement, considering the many refinements omitted from the calculations. The ionization data for Hf^{3+} indicate that f-subshell electrons ionize less effectively than those in other subshells, consistent with the estimates using the SPWBA methods of McGuire.[14]

ACKNOWLEDGMENTS

The authors would like to acknowledge R. A. Phaneuf for providing valuable consultation on the experiment. J. W. Hale provided significant technical assistance in the ion-source development. This work was supported in part by the Office of Fusion Energy, U.S. Department of Energy.

---

*Staff member, Quantum Physics Division, National Bureau of Standards.

[1]B. Peart and K. Dolder, J. Phys. B 1, 872 (1968); 8, 56 (1975); B. Peart, J. G. Stevenson, and K. Dodler, *ibid.* 6, 146 (1973).

[2]R. K. Feeney, J. W. Hooper, and M. T. Elford, Phys. Rev. A 6, 1469 (1972); M. T. Elford, R. K. Feeney, and J. W. Hooper, *Proceedings of the Sixth ICPEAC,* edited by I. Amdur (MIT, Cambridge, Mass., 1969), p. 620.

[3]R. A. Falk, G. H. Dunn, D. C. Griffin, C. Bottcher, D. C. Gregory, and D. H. Crandall, Phys. Rev. Lett. 47, 494 (1981).

[4]For example, see L. Goldberg, A. K. Dupree, and J. W. Allen, Ann. Astrophys. 28, 589 (1965); J. W. Allen and A. K. Dupree, Astrophys. J. 155, 27 (1969); C. Jordan, Mon. Not. R. Astron. Soc. 142, 501 (1969); H. Nussbaumer and P. J. Storey, Astron. Astrophys. 44, 321 (1975); V. L. Jacobs, J. Davis, P. C. Kepple, and M. Blaha, Astrophys. J. 211, 605 (1977); O. Bely, Ann. Astrophys. 30, 953 (1967); Y. Hahn, Phys. Rev. Lett. 39, 82 (1977); Y. Hahn, Phys. Rev. A 18, 1028 (1978); R. D. Cowan and J. B. Mann, Astrophys. J. 232, 940 (1978).

[5]D. C. Griffin, C. Bottcher, and M. S. Pindzola, Phys. Rev. A 25, 1374 (1982).

[6]D. H. Crandall, R. A. Phaneuf, and P. O. Taylor, Phys. Rev. A 18, 1911 (1978).

[7]Some reviews: M. F. A. Harrison, J. Appl. Phys. 17, 371 (1966); G. H. Dunn, in *Atomic Physics,* edited by V. W. Hughes, V. W. Cohen, and F. M. S. Pichanick (Plenum, New York, 1969), p. 417; K. T. Dolder and B. Peart, Rep. Prog. Phys. 39, 693 (1976).

[8]P. O. Taylor, K. T. Dodler, W. E. Kauppila, and G. H. Dunn, Rev. Sci. Instrum. 45, 538 (1974).

[9]M. L. Mallory and D. H. Crandall, IEEE Trans. Nucl. Sci. NS-23, 1069 (1976).

[10]W. Lotz, Astrophys. J. Suppl. 14, 207 (1967); W. Lotz, Z. Phys. 216, 241 (1968); 220, 466 (1969); 206, 205 (1967).

[11]D. C. Griffin, C. Bottcher, and M. Pindzola (private communication).

[12]K. J. LaGattuta and Y. Hahn, Phys. Rev. A 24, 2273 (1981).

[13]R. J. W. Henry and A. Msezane, Phys. Rev. A 26, 2545 (1982).

[14]E. J. McGuire, Phys. Rev. A 16, 73 (1977); 20, 445 (1979).

[15]L. B. Golden and D. H. Sampson, J. Phys. B 13, 2645 (1980).

[16]D. H. Crandall, Phys. Scr. 23, 153 (1981); D. H. Crandall, R. A. Phaneuf, B. E. Hasselquist, and D. C. Gregory, J. Phys. B 12, L249 (1979); D. H. Crandall, R. A. Phaneuf, and D. C. Gregory, Report No. ORNL/TM-7020 Oak Ridge National Laboratory, Tennessee (un-

published); G. H. Dunn, in *The Physics of Ionized Gases*, edited by M. Matić (Boris Kidrić Institue of Nuclear Sciences, Belgrade, 1980), pp. 49–95; D. H. Crandall, R. A. Phaneuf, R. A. Falk, D. S. Belic, and G. H. Dunn, Phys. Rev. A 25, 143 (1982).

[17]D. C. Griffin (private communication).

[18]W. T. Rogers, G. Stefani, R. Camilloni, G. H. Dunn, A. Z. Msezane, and R. J. W. Henry, Phys. Rev. A 25, 737 (1982).

[19]D. Belić, R. A. Falk, C. Timmer, and G. H. Dunn, unpublished work on ionization of Hg^+ and Cd^+.